

Design and fabrication of high-index-contrast self-assembled texture for light extraction enhancement in LEDs

Xing Sheng,^{1,*} Lirong Zeng Broderick,¹ Juejun Hu,² Li Yang,³ Anat Eshed,¹ Eugene A. Fitzgerald,¹ Jurgen Michel,¹ and Lionel C. Kimerling¹

¹Department of Materials Science and Engineering, Massachusetts Institute of Technology, Cambridge, Massachusetts 02139, USA

²Department of Materials Science and Engineering, University of Delaware, Newark, Delaware 19716, USA

³Department of Physics, Massachusetts Institute of Technology, Cambridge, Massachusetts 02139, USA
*shengx@mit.edu

Abstract: We developed a high-index-contrast photonic structure for improving the light extraction efficiency of light-emitting diodes (LEDs) by a self-assembly approach. In this approach, a two-dimensional grating can be non-lithographically integrated on the top of virtually any types of LEDs with controlled structural parameters and material indices. As a proof of concept, our designed photonic structure was implemented on a GaAs double heterojunction LED. Using numerical electromagnetic simulations, we explored the effects of the structural parameters (the grating period, layer thickness and material indices) on the device performances, followed by fabrication through a self-assembled porous alumina as a template. Device simulation and experimental results indicate that an optimized high-index-contrast (a-Si / air) grating obtains a much larger efficiency increase than using a low-index SiO₂ grating. In addition, the devices maintain a Lambertian radiation pattern with the self-assembled grating. This technique provides an effective and low-cost method for improving LED efficiency.

©2011 Optical Society of America

OCIS codes: (250.0250) Optoelectronics; (230.3670) Light-emitting diodes.

References and links

1. M. R. Krames, O. B. Shchekin, R. Mueller-Mach, G. O. Mueller, L. Zhou, G. Harbers, and M. G. Craford, "Status and future of high-power light-emitting diodes for solid-state lighting," *J. Display Technol.* **3**(2), 160–175 (2007), <http://www.opticsinfobase.org/jdt/abstract.cfm?URI=jdt-3-2-160>.
2. I. Schnitzer, E. Yablonovitch, C. Caneau, and T. J. Gmitter, "Ultrahigh spontaneous emission quantum efficiency, 99.7% internally and 72% externally, from AlGaAs/GaAs/AlGaAs double heterostructures," *Appl. Phys. Lett.* **62**(2), 131–133 (1993), <http://link.aip.org/link/doi/10.1063/1.109348>.
3. E. Schubert, *Light Emitting Diodes*, (Cambridge University Press, 2006).
4. C. J. Nuese, J. J. Tietjen, J. J. Gannon, and H. F. Gossenberger, "Optimization of electroluminescent efficiencies for vapor-grown GaAs_{1-x}P_x diodes," *J. Electrochem. Soc.* **116**(2), 248–253 (1969), <http://dx.doi.org/10.1149/1.2411807>.
5. O. B. Shchekin, J. E. Epler, T. A. Trotter, T. Margalith, D. A. Steigerwald, M. O. Holcomb, P. S. Martin, and M. R. Krames, "High performance thin-film flip-chip InGaN–GaN light-emitting diodes," *Appl. Phys. Lett.* **89**(7), 071109 (2006), <http://link.aip.org/link/doi/10.1063/1.2337007>.
6. T. Fujii, Y. Gao, R. Sharma, E. L. Hu, S. P. DenBaars, and S. Nakamura, "Increase in the extraction efficiency of GaN-based light-emitting diodes via surface roughening," *Appl. Phys. Lett.* **84**(6), 855–857 (2004), <http://link.aip.org/link/doi/10.1063/1.1645992>.
7. H. S. Yang, S. Y. Han, K. H. Baik, S. J. Pearton, and F. Ren, "Effect of inductively coupled plasma damage on performance of GaN-InGaN multiquantum-well light-emitting diodes," *Appl. Phys. Lett.* **86**(10), 102104 (2005), <http://link.aip.org/link/doi/10.1063/1.1882749>.
8. S. Fan, P. R. Villeneuve, J. D. Joannopoulos, and E. F. Schubert, "High extraction efficiency of spontaneous emission from slabs of photonic crystals," *Phys. Rev. Lett.* **78**(17), 3294–3297 (1997), <http://link.aps.org/doi/10.1103/PhysRevLett.78.3294>.
9. A. A. Erchak, D. J. Ripin, S. Fan, P. Rakich, J. D. Joannopoulos, E. P. Ippen, G. S. Petrich, and L. A. Kolodziejski, "Enhanced coupling to vertical radiation using a two-dimensional photonic crystal in a semiconductor light-emitting diode," *Appl. Phys. Lett.* **78**(5), 563–565 (2001), <http://link.aip.org/link/doi/10.1063/1.1342048>.

10. E. Matioli, E. Rangel, M. Iza, B. Fleury, N. Pfaff, J. Speck, E. Hu, and C. Weisbuch, "High extraction efficiency light-emitting diodes based on embedded air-gap photonic-crystals," *Appl. Phys. Lett.* **96**(3), 031108 (2010), <http://link.aip.org/link/doi/10.1063/1.3293442>.
11. J. J. Wierer, A. David, and M. M. Megens, "III-nitride photonic-crystal light-emitting diodes with high extraction efficiency," *Nat. Photonics* **3**(3), 163–169 (2009), <http://www.nature.com/nphoton/journal/v3/n3/full/nphoton.2009.21.html>.
12. M. Fujita, S. Takahashi, Y. Tanaka, T. Asano, and S. Noda, "Simultaneous inhibition and redistribution of spontaneous light emission in photonic crystals," *Science* **308**(5726), 1296–1298 (2005), <http://www.sciencemag.org/content/308/5726/1296> (abstract).
13. D. Delbeke, P. Bienstman, R. Bockstaele, and R. Baets, "Rigorous electromagnetic analysis of dipole emission in periodically corrugated layers: the grating-assisted resonant-cavity light-emitting diode," *J. Opt. Soc. Am. A* **19**(5), 871–880 (2002), <http://www.opticsinfobase.org/abstract.cfm?URI=josaa-19-5-871>.
14. E. Palik, *Handbook of Optical Constants of Solids* (Academic Press, 1998).
15. C. F. Lai, J. Y. Chi, H. C. Kuo, H. H. Yen, C. E. Lee, C. H. Chao, W. Y. Yeh, and T. C. Lu, "far-field and near-field distribution of GaN-based photonic crystal LEDs with guided mode extraction," *IEEE J. Sel. Top. Quantum Electron.* **15**(4), 1234–1241 (2009), <http://dx.doi.org/10.1109/JSTQE.2009.2015582>.
16. K. Kim, J. Choi, T. S. Bae, M. Jung, and D. H. Woo, "Enhanced light extraction from nanoporous surfaces of InGaN/GaN-based light emitting diodes," *Jpn. J. Appl. Phys.* **46**(No. 10A), 6682–6684 (2007), <http://jjap.jsap.jp/link?JJAP/46/6682/>.
17. C. C. Liu, S. X. Lin, C. C. Wang, K. K. Chong, C. I. Hung, and M. P. Houng, "Light output enhancement of AlGaInP light emitting diodes with nanopores of anodic alumina," *Jpn. J. Appl. Phys.* **48**(8), 082102–082104 (2009), <http://jjap.jsap.jp/link?JJAP/48/082102/>.
18. X. Sheng, J. Liu, I. Kozinsky, A. M. Agarwal, J. Michel, and L. C. Kimerling, "Design and non-lithographic fabrication of light trapping structures for thin film silicon solar cells," *Adv. Mater. (Deerfield Beach Fla.)* **23**(7), 843–847 (2011), <http://onlinelibrary.wiley.com/doi/10.1002/adma.201003217/abstract>.
19. T. Egawa, Y. Niwano, K. Fujita, K. Nitatori, T. Watanabe, T. Jimbo, and M. Umeno, "First fabrication of AlGaAs/GaAs double-heterostructure light-emitting diodes grown on GaAs(111)a substrates using only silicon dopant," *Jpn. J. Appl. Phys.* **34**(Part 1, No. 2B), 1270–1272 (1995), <http://jjap.jsap.jp/link?JJAP/34/1270/>.
20. W. H. Koo, S. M. Jeong, F. Araoka, K. Ishikawa, S. Nishimura, T. Toyooka, and H. Takezoe, "Light extraction from organic light-emitting diodes enhanced by spontaneously formed buckles," *Nat. Photonics* **4**(4), 222–226 (2010), <http://www.nature.com/nphoton/journal/v4/n4/abs/nphoton.2010.7.html>.
21. H. Masuda and K. Fukuda, "Ordered metal nanohole arrays made by a two-step replication of honeycomb structures of anodic alumina," *Science* **268**(5216), 1466–1468 (1995), <http://www.sciencemag.org/content/268/5216/1466.short>.

1. Introduction

Light-emitting diodes (LEDs) have become an emerging and promising candidate for light sources. Unlike conventional incandescent or fluorescent light sources, LEDs directly transfer electricity into light. Therefore, it has many advantages such as high energy conversion efficiency, long lifetime and small footprint [1]. Typical LED devices are made of inorganic (III-V) or organic semiconductor junctions. The internal quantum efficiency η_i of the light emission process, which is the portion of electron-hole pairs converted into photons, can be increased by improving material quality, and the state-of-the-art η_i has reached 90%, already approaching the theoretical limit [2]. As a consequence, currently the major LED efficiency limiting factor becomes poor light extraction, i.e. photons trapped inside the device due to total internal reflection at semiconductor and air interface. For a planar LED, the light extraction efficiency η_e can be estimated to be $1/4n^2$ [3]. For most semiconductors, their refractive indices n are high ($n > 2$). Therefore, η_e is a severe limitation for overall device performance.

To resolve the issue of limited extraction efficiency η_e in semiconductor LEDs, many photonic designs have been proposed. For example, organic materials are used as encapsulants to cover the top surface and reduce the total internal reflection [4]. Another example is to roughen/texture the device surface and induce stronger scattering effect [5,6]. However, these methods have limitations. Organic encapsulants suffer from degradation under photon radiation (especially for blue and green light), which largely limits their use for long lifetime and high brightness LEDs. Texturing semiconductor surface (by plasma etching, for example) generates defects that work as recombination centers that exacerbate non-radiative recombination and decrease the internal quantum efficiency η_i [7]. Furthermore, random scattering surfaces generated using a conventional texturing process lack the ability to purposefully optimize and control the structural parameters of the textured surface.

Photonic crystal (PhC) has a structure with one, two, or three dimensional (1D, 2D and 3D) periodic patterns consisting of two materials with different refractive indices. In such periodic structures, light propagation can be controlled in various ways [8,9]. To increase LED extraction efficiency, a two-dimensional photonic crystal structure can be embedded in the device [10] or integrated on top surface [11,12]. Due to the periodicity, the guided waves can leak to free space as Bloch modes. Therefore, light can escape from the high index semiconductors even if the incident angle is larger than the critical angle. However, to fabricate these photonic crystals with submicron feature size, high-cost methods like interference lithography or electron beam lithography have to be employed, which prohibits LED cost reduction and high-volume production. Therefore, a low-cost and controllable method is highly desirable for fabrication of light extraction photonic crystal structures in LED devices.

Here, we proposed a self-assembled two-dimensional photonic structure to increase the light extraction efficiency in LEDs. The proposed structure has several advantages: (1) A potentially low-cost, self-assembled method is introduced for fabrication, and the structural parameters can be controlled by experimental conditions; (2) Unlike plasma or wet chemical etching, the method is non-specific and can be implemented on top of any semiconductors; (3) Instead of etching through the active device, the structure is directly deposited on the surface, so it is non-damaging and does not cause any degradation of internal quantum efficiency η_i ; (4) According to the targeted emission wavelength, various materials can be deposited to make the structure for achieving optimal light extraction; (5) As we will discuss below, a high-index-contrast texture is used, which provides much more efficient light extraction than low-index-contrast structures like SiO_2 / air or Al_2O_3 / air gratings.

We organize the paper as follows: Section 2 described a p-AlGaAs / i-GaAs / n-AlGaAs double heterojunction LED used in our experiments. Section 3 numerically explored the effects of the structural parameters as well as material index contrast for the proposed structure. The self-assembled technique for grating fabrication is shown in Section 4. In Section 5, we analyzed the performances of the light extraction structures. By using the optimized high-index-contrast grating, the light emission intensity is improved by 27%. Here we want to point out that even though similar 2D grating designs have been applied to increase light extraction in LEDs, the gratings used in previous reports are low-index gratings. As we show in Sections 3 and 5, such low-index gratings have inherently limited light extraction capabilities. In contrast, our self-assembly processing is highly flexible in grating material selection and thus enables significant extraction enhancement using high-index gratings.

2. Device structure

The proposed photonic structure is integrated onto a conventional GaAs based LED, as shown in Fig. 1(a). A double heterojunction was grown on an n-type GaAs substrate by Metal-Organic Chemical Vapor Deposition (MOCVD). The detailed structure (from bottom to top) is 1 μm n- $\text{Al}_{0.3}\text{Ga}_{0.7}\text{As}$ (Si doping, $n = 4 \times 10^{18} \text{ cm}^{-3}$), 0.12 μm intrinsic GaAs and 1 μm p- $\text{Al}_{0.3}\text{Ga}_{0.7}\text{As}$ (Zn doping, $p = 4 \times 10^{18} \text{ cm}^{-3}$). Subsequently, a thin p-GaAs layer (200nm, Zn doping, $p = 1 \times 10^{19} \text{ cm}^{-3}$) is grown on top of the p-i-n junction as a protecting layer to prevent the $\text{Al}_{0.3}\text{Ga}_{0.7}\text{As}$ layer from oxidation and enable a better ohmic contact. Ideal ohmic contacts on the n-GaAs and p-GaAs are formed by 20 nm Ni / 30 nm Ge / 200 nm Au and 20 nm Ni / 30 nm Zn / 200 nm Au, followed by rapid thermal annealing (at 400 °C for 40 seconds). The above procedures create the reference LED device without light extraction structures.

The top view of designed light extraction configuration is plotted in Fig. 1(b), made by a hexagonal pattern as a grating layer. Due to the diffraction effect of the grating, light propagating at oblique angles (outside the emission cone) can be partly coupled out from the high index III-V semiconductor layer. Therefore, the light extraction efficiency will be significantly improved. Since the light out-coupling critically depends on the light extraction

structure, the grating should be carefully designed to maximize the efficiency at the device emission wavelength.

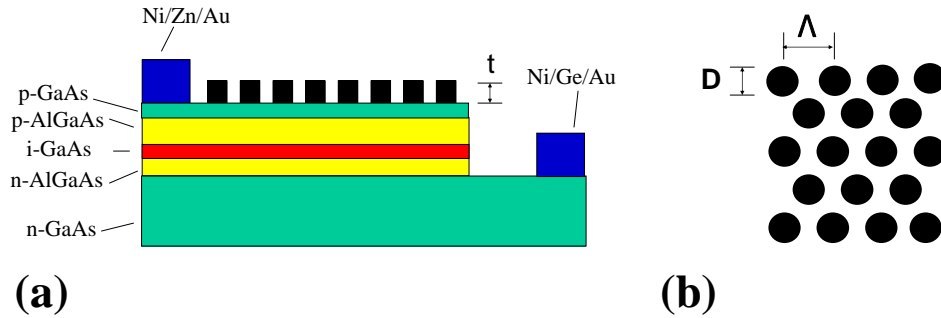


Fig. 1. (a) Schematic layout of a test LED device with photonic crystal structures integrated on top surface for light extraction. The active device is a double heterojunction based on a GaAs substrate. (b) Top view of the photonic crystal layer, which has a hexagonal lattice, with period A , thickness t and rod diameter D .

3. Numerical simulation

3.1 Optimization of grating parameters

A three-dimensional model based on rigorous coupled wave analysis (RCWA) was utilized to optimize the performance of the grating design. The basic theory can be found in the reference [13]. The simulated device structure used in this model is described in the previous section, excluding the metallic contact pads. The optical properties (refractive index n and extinction coefficient k) for all the materials are quoted from E. Palik [14]. The simulation is performed at the central emission wavelength, which is 870 nm corresponding to the bandgap of GaAs ($E_g = 1.43$ eV). A monochromatic dipole is placed in the middle of the intrinsic GaAs layer and the emitting field intensity on top of the grating layer is integrated over all angles to calculate the extraction efficiency. Unlike nitride based semiconductor, GaAs has a zinc blende structure, which leads to an isotropic spontaneous emission. Therefore, the overall extraction efficiency is averaged over different dipole orientations and dipole positions with respect to the grating unit cell.

Here we show that the structure and optical parameters of the gratings (refractive index, grating period A , cylinder diameter D and thickness t in Fig. 1(b)) can significantly impact the light extraction efficiency. Here we assume the grating filling area ratio is 1:1, i.e., $D = 0.74 A$, and study the impact of varying A and t . To quantify the effect of grating index contrast, we simulated two types of gratings, amorphous silicon (a-Si) in air matrix and silicon dioxide (SiO_2) in air matrix. Figure 2(a) and 2(b) plot the relative LED efficiency enhancement as functions of A and t for both types of gratings. Figure 2(a) reveals that when we choose appropriate values (A and t) for the a-Si / air grating, strong light extraction effect appears and the LED performance is enhanced. According to the simulation, the optimized design corresponds to $A = 500$ nm and $t = 200$ nm, where an enhancement factor of up to 70% can be achieved. Although the SiO_2 / air grating has a similar optimized region ($A = 600$ nm and $t = 250$ nm), the optimal enhancement factor is much lower (about 18%). This suggests that the a-Si / air grating is very effective in enhancing light extraction, because of the high index contrast (4.0 versus 1.0) of this system as well as the transparency of a-Si in the near-infrared wavelength range. In comparison, the optimal enhancement is far less significant in the SiO_2 / air grating design (Fig. 2(b)) due to the much lower index contrast (1.4 versus 1.0).

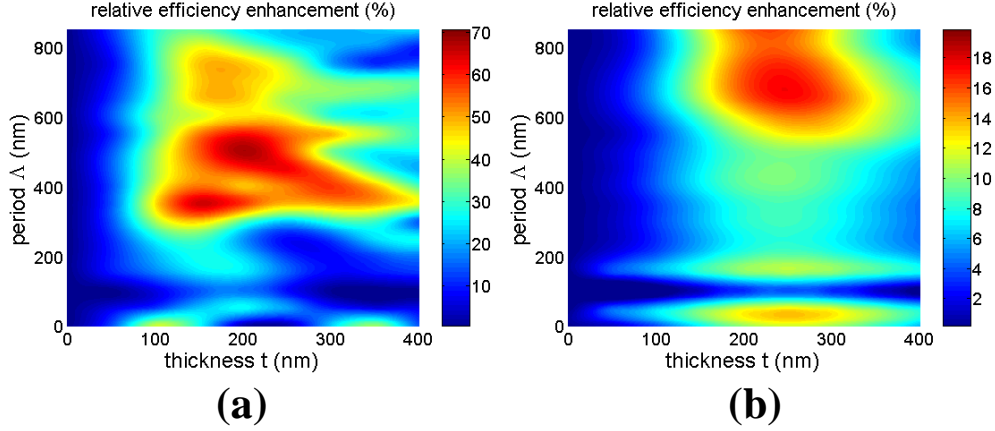


Fig. 2. Plot of the relative efficiency increase after introducing the grating layer for light extraction, as a function of grating period Δ and thickness t . The performance is compared with the planar device without the grating. Grating structure: (a) a-Si hexagonal pattern in air matrix; (b) SiO₂ hexagonal pattern in air matrix.

3.2 Calculation of far field emission profiles

To further understand the effects of high-index-contrast grating, we analyzed the far field emission pattern for the LED structure with the optimal grating parameters (a-Si / air grating with $\Delta = 500$ nm and $t = 200$ nm). Figure 3 compares the contour plots for the LEDs with and without grating in the reciprocal space. In Fig. 3(a) and 3(b), k_x and k_y are parallel to the device plane, and each point (k_x, k_y) corresponds to a specific emission angle θ in the far field,

$$\sin \theta = \frac{\sqrt{k_x^2 + k_y^2}}{2\pi / \lambda_0} = \frac{\sqrt{k_x^2 + k_y^2}}{k_0} \quad (1)$$

The averaged angular dependences are plotted in Fig. 3(c). As expected, the planar device reveals a Lambertian emission pattern with a maximum in the normal direction, since GaAs has an isotropic spontaneous emission. For the LED with grating, the non-Lambertian behavior is caused by the outcoupling of the guided modes due to diffraction, which also explains the improvement of extraction efficiency. Because the results are averaged among dipoles emitting at different directions and combining both TE and TM modes, no significantly sharp peaks can be observed as mentioned in some references [11,15].

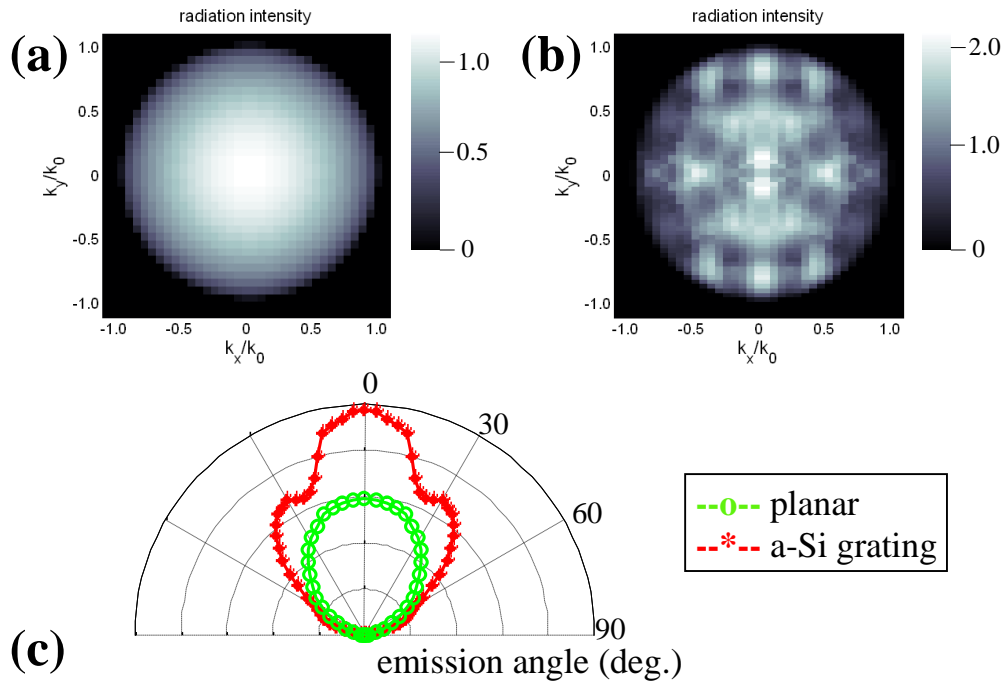


Fig. 3. Simulated far-field emission pattern at a wavelength of 870 nm. (a) Planar LED without grating on top, which shows a Lambertian pattern. (b) LED with a periodic a-Si / air grating of optimized parameters ($A = 500$ nm and $t = 200$ nm), which shows a non-Lambertian pattern. (c) Averaged angular dependence of light emission for devices without (green) and with (red) a-Si grating. The normalized intensity has an arbitrary unit.

4. Fabrication and characterization of the self-assembled light extraction structures

The above simulation results predict and optimize the performance of devices with a perfectly periodic texture. To fabricate the optimized sub-micron light extraction structure on top of the LED devices, one needs to resort to lithographic techniques. If the light extraction structure only has short range order, the device performances will deviate from the simulations because of the average effect due to imperfection. However, the influences of different index contrast can still be observable in those short-range-order structures.

To demonstrate the effect of refractive index contrast on extraction efficiency, we use low-cost, self-assembled anodic aluminum oxide (AAO) templates as an alternative to high resolution lithography. AAO has a highly porous structure, of which the feature size (inter-pore distance, pore size, etc.) can be modulated by the anodization condition, and it has been used directly as light extraction structures in some previous work [16,17]. However, as we demonstrated in the above simulations, the low index contrast between air and alumina (1.0 versus 1.7) will significantly limit the extraction enhancement. Also, the electrolyte used in the anodization process can severely degrade the active device by introducing surface defects. To overcome these challenges of directly using AAO for light extraction, we used AAO as a template. Details of the process can be referenced in [18]. By a two-step anodization at a constant DC voltage of 200 V in a 1.0 M citric acid solution, self-organized AAO with a uniform pore distribution can be fabricated and used as a deposition mask. Figure 4(a) shows a SEM image of a fabricated AAO membrane with a period of about 500 nm and thickness of nearly 1 μm . Through this thin porous membrane, various materials including semiconductors and metals can be deposited via simple thermal or electron beam evaporation. As we designed in the previous section, 200 nm a-Si and SiO_2 are deposited on top of the GaAs LEDs respectively, forming the optimal designed light extraction structure. Shown in the AFM

images (Fig. 4(b) and 4(c)), the deposited a-Si and SiO₂ pattern have very similar morphology, directly replicating the near hexagonal AAO pore arrays.

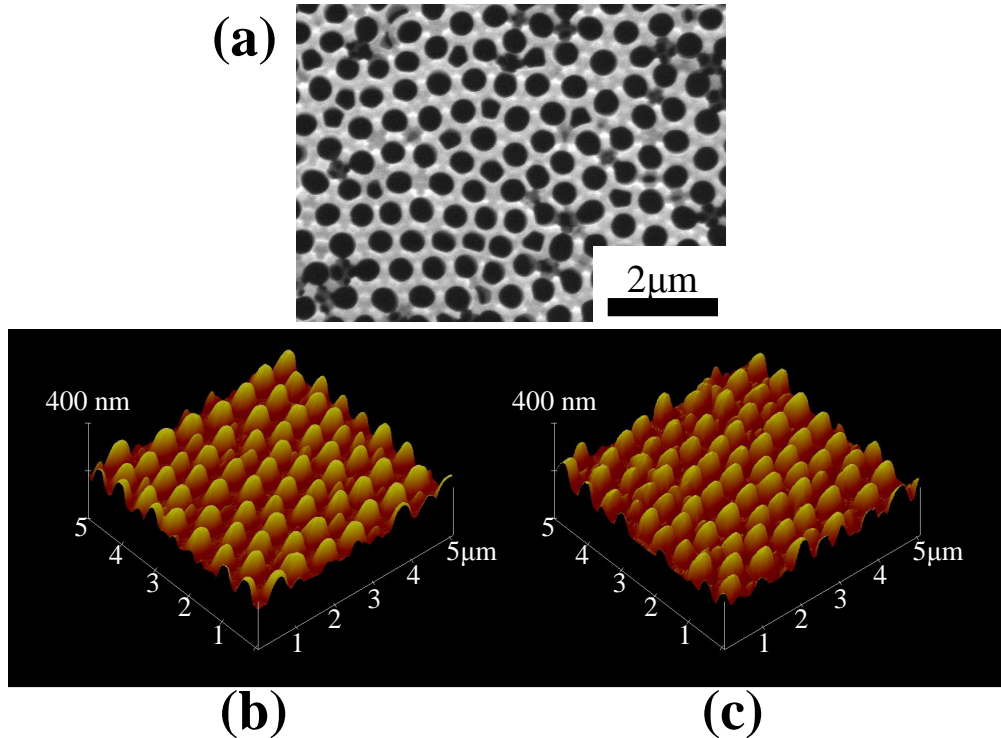


Fig. 4. (a) SEM image of the anodized porous alumina membrane utilized as a deposition mask; (b) AFM image of the deposited a-Si pattern; (c) AFM image of the deposited SiO₂ pattern.

5. Experimental results and discussion

The electroluminescence (EL) performances of LEDs with different light extraction structures were measured using an optical multimeter (Ando AQ2140). A multimode fiber (100 μm diameter, NA = 0.28) was placed above the devices to collect the emitted photons from the surface. The light intensity-current (*L-I*) characteristics are shown in Fig. 5(a). The slight non-linear behavior is due to some feedback mechanisms, causing a small portion of stimulated emission [19]. It can be clearly seen that the emission intensity is significantly higher if the designed grating is used as a light extraction structure. Compared to the planar device without any light extraction structure, the device with a-Si grating shows a relative efficiency improvement of 27%, while the SiO₂ grating only achieves 7.3% relative increase. These results are further confirmed by the emission spectra measured under a current of 20 mA by an optical spectrum analyzer (Ando AQ6315A). As illustrated in Fig. 5(b), all the spectra peak at 870 nm, with a full width at half-maximum (FWHM) of 26 nm. The *L-I* curves and emission spectra clearly reveal that the grating with higher index contrast entails higher performance for light extraction, which agrees well with our numerical predictions. Other approaches show a 130% increase in GaN devices by surface roughening [6] and 39% increase in AlGaInP directly using the low-index AAO [17]. The differences in materials systems (GaAs vs. GaN or AlGaInP) and device configurations (bulk vs. thin film) lead to lower efficiency improvements in our case. However, our approach can be implemented in those different systems and will yield better performances which scale with index-contrast and structural parameters according to our model.

Figure 5(c) shows the angular dependence of emission for the devices with and without a-Si grating. In the measurement, the devices are mounted on a goniometer which can rotate 90 degrees. Unexpectedly, both the devices show a Lambertian emission pattern, which does not fully agree with the simulation predictions shown in Fig. 3(c). This is mainly due to the imperfection of the fabricated grating. As seen in the SEM image of AAO membrane (Fig. 4(a)), the pore distribution only exhibits short-range order. In addition, the AFM images of the deposited a-Si and SiO₂ indicate we obtained a cone-shaped array. Therefore, the self-assembled approach causes a deviation from the ideal hexagonal array of cylinders, thus inducing random scattering and forming the near-Lambertian emission pattern [20].

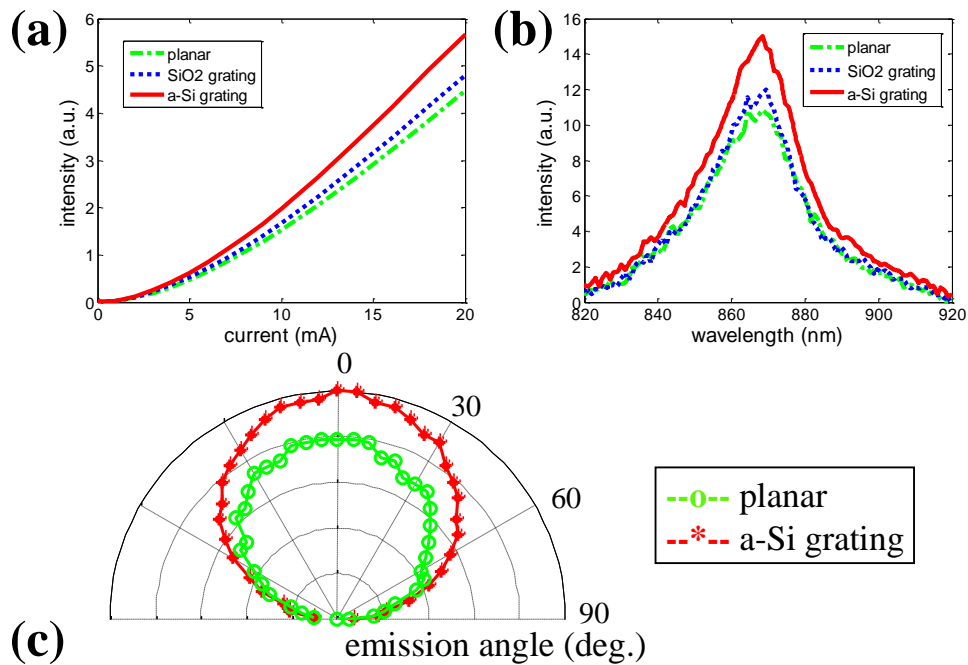


Fig. 5. Performances for LED devices with various top structures: the planar LED without grating (green), the LED with SiO₂ grating (blue) and the LED with a-Si grating (red). (a) Light intensity-current ($L-I$) curves; (b) Emission spectra measured at current of 20 mA. It can be observed that the LED with a-Si grating shows the highest emission intensity, thus obtaining the highest efficiency. (c) Angular resolved measurement of light emission for the planar LED and the one with a-Si grating. The normalized intensity has an arbitrary unit.

Although the above results are obtained from GaAs based near-IR LEDs, the proposed design can also be applied for light extraction in LEDs emitting at other spectral ranges. For visible LEDs based on nitride or organic semiconductors, the simulation and fabrication methods we utilized here are still applicable, while the structural parameters should be altered to accommodate the target wavelength. The AAO template has controllable feature sizes, which can be manipulated by varying experimental conditions like applied voltage and anodization time [21]. It should be noted that a-Si becomes strongly absorptive at visible wavelengths (< 700 nm). Therefore, other materials should be exploited to make the self-assembled pattern. Possible candidates can be SiC and ZnS, both of which have high refractive indices as well as low absorption coefficients in the visible range [14].

6. Conclusion

In this paper, a self-assembled light extraction structure was integrated for LED efficiency enhancement. Based on numerical simulations, we systematically investigated the impact of grating parameters and materials selection on the light extraction. We showed that high-index

gratings are far more effective in light extraction improvement compared to their low-index counterpart. The optimized structures were integrated on GaAs based LEDs by using self-assembled AAO membranes as a template, which acts as an effective and low-cost alternative to lithographic fabrications. The LED device with the optimized high-index-contrast a-Si grating yielded a 27% improvement in emission intensity. The effects of different index contrasts were verified by comparing the performances of gratings made from a-Si and SiO₂. Unlike the simulation results, the device with fabricated a-Si grating showed a Lambertian emission pattern, which is due to the non-ideality of the periodicity. By proper structure design and materials selection, these approaches could also provide a guideline for efficiency enhancement in nitride and organic based LEDs.

Acknowledgments

The authors would like to thank Massachusetts Institute of Technology Energy Initiative (MITEI) Seed Fund Program for financial support.